The $\pi-\pi$ Stacked Geometries and Association Thermodynamics of Quinacridone Derivatives Studied by ^{1}H NMR

Hui Sun, Kaiqi Ye, Chunyu Wang, Haiyan Qi, Fei Li,* and Yue Wang*

Key Laboratory for Supramolecular Structure and Materials of Ministry of Education, Jilin University, Changchun 130012, People's Republic of China

Received: December 12, 2005; In Final Form: July 11, 2006

The $\pi-\pi$ stacked associations of three *N*,*N*′-di(*n*-butyl) quinacridone derivatives, widely used dopants in organic light-emitting diodes, with different sizes of substituents were investigated in solution at various temperatures by ^{1}H NMR spectroscopy. The $\pi-\pi$ stacked geometries were estimated by both the magnitudes of peak shifts with concentration and the directions of peak shifts induced by polar solvents. Two patterns of geometries with different $\pi-\pi$ interaction strengths were found to coexist in solution for all the three samples. In both of the patterns, the preferential orientation of the stacking is the approach of the carbonyl groups on one molecule to the nitrogen atoms on the stacked partner, which makes the π-deficient aromatic atoms interact with both π-rich and π-deficient aromatic atoms of the stacked partner to maximize the electrostatic complementarity. Differently, whereas the molecules in one pattern are face-to-face stacked in a parallel fashion and slip two rings relative to one another along with the long axis of the conjugated ring systems, the molecules in the other are either face-to-face stacked in an antiparallel fashion with slight slipping between layers or stacked in a turning fashion. Both association constants obtained by fitting the dilution curves and thermodynamic parameters obtained from van't Hoff analyses revealed unexpectedly three thermodynamic processes of aggregations for all the three samples in the temperature region of 298−213 K. The size of substituents on the outer aromatic rings significantly influences the $\pi-\pi$ stacked structures and association thermodynamics.

Introduction

Aggregation effects may change the properties of materials, for example, color of a pigment and the performance of electroluminescent device. Thus, it is no longer sufficient for the organic chemists to synthesize new compounds. They must consider how these materials organize themselves in solution or in the solid state and how to control that organization. The manner of the organization is also important for the structures and functions of biomolecules. The $\pi-\pi$ stacked aromatic interactions have been found to govern diverse supramolecular organizations and aggregates in both the solution and the solid state.[1] They not only control the vertical base−base stacking in DNA[2,3] and the tertiary structures of proteins[4−6] but also play a major role in the assembly and crystallization based on many synthetic molecules.[7−12] Theoretical calculations for a limited number of systems[13−17] and NMR experiments for many polyaromatic molecules[6−10,18−22] have been carried out to get insight into the origin and geometrical preference of the $\pi-\pi$ stacked interaction. However, in comparison to more conventional interactions such as hydrogen bonds, ion pairs (salt bridges), and hydrophobic interaction, the $\pi-\pi$ stacked interaction is not so clear, and to date, no commonly used model has been built to interpret the experimental observations well. This should be attributed to the complication of the $\pi-\pi$ stacked interaction, e.g., multiple points of intermolecular contact, strong dependency on substituent groups, variable geometries, and the cooperative effect of various noncovalent interactions.[1] Therefore, the study on the variety of systems involved in the $\pi-\pi$ stacked interaction is an important step toward a full understanding of this type of noncovalent interaction.

N,*N*′-dialkylated quinacridone derivatives have been used as dopants in electroluminescent devices for their high photoluminescent efficiency in dilute solution and good electrochemical stability in the solid state.[23−26] It was found that the EL device based on the Alq_3 thin film doped with *N*,*N*′-di(*n*-butyl) quinacridone displayed high efficiency (>10 cd/A) within only a narrow concentration range from 0.5% to 1.0%, while the EL device based on the Alq_3 thin film doped with *N*,*N*′-di(*n*-butyl)-1,3,8,10-tetramethyl quinacridone exhibited high efficiency (>10 cd/A) for a wider concentration range from 0.5% to 5.0%. Moreover, the Alq_3 thin films doped with *N*,*N*′-di(*n*-butyl) quinacridone and *N*,*N*′-di(*n*-butyl)-1,3,8,10-tetramethyl quinacridone displayed PL quenching when the concentrations of the two dopants reached 4.2% and 6.7%, respectively. The different PL and EL concentration-dependent properties of the doped Alq_3 solid thin films were attributed to the different molecular packing characteristics of the two dopants in the solid state. The study by X-ray crystallography showed that both the *N*,*N*′-di(*n*-butyl) quinacridone and *N*,*N*′-di(*n*-butyl)-1,3,8,10-tetramethyl quinacridone formed the intermolecular $\pi-\pi$ stacking in the solid state and the latter had a smaller stacking density than the former. The smaller stacking density of *N*,*N*′-di(*n*-butyl)-1,3,8,-10-tetramethyl quinacridone decreases the PL and EL quenching arising from the $\pi-\pi$ interaction and thus maintains the PL and EL efficiency of the doped Alq_3 thin film at a high level in a wider range of dopant concentration.[26] Therefore, the control of molecular packing in the solid state by design of molecular structure is meaningful for improving the performance of the EL device. Because the $\pi-\pi$ interaction plays an important role in the packing of dopants, the investigation of the $\pi-\pi$ stacked

10.1021/jp057232a CCC: $33.50
Published on Web 08/26/2006

SCHEME 1: Structures of Three *N*,*N*′-di(*n*-Butyl) Quinacridone Derivatives

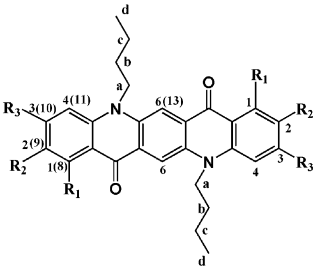

DBQA: $R_1=R_2=R_3=H$

TM-DBQA: $R_1=R_3=-CH_3$, $R_2=H$

D^{t}Bu-DBQA: $R_2=-C(CH_3)_3$, $R_1=R_3=H$

interaction is helpful for the design of luminescent molecules with desired assembly properties.

Here, we use ^{1}H NMR spectroscopy to study the $\pi-\pi$ stacked aggregations and aggregation thermodynamics of three *N*,*N*′-di(*n*-butyl) quinacridone derivatives with different sizes of substituents on the outer aromatic rings, namely, *N*,*N*′-di(*n*-butyl) quinacridone (DBQA), *N*,*N*′-di(*n*-butyl)-1,3,8,10-tetramethyl quinacridone (TM−DBQA), and *N*,*N*′-di(*n*-butyl)-2,9-di(*tert*-butyl) quinacridone (D^{t}Bu−DBQA), in solution at various temperatures. Their $\pi-\pi$ stacked geometries in solution were first estimated by both the magnitudes of the peak shifts of protons at different positions of the molecules with concentration and the directions of these peak shifts induced by polar solvents.

Materials and Methods

Quinacridone was purchased from Tokyo Kasei Kogyo Company. 3,5-Dimethylaniline and 1-bromobutane were obtained from Acros Organics. Diethyl-2,5-dihydroxy-1,4-dicarboxylate was purchased from Aldrich. The chemicals were used directly without further purification.

N,*N*′-di(*n*-butyl) quinacridone (DBQA), *N*,*N*′-di(*n*-butyl)-1,3,8,10-tetramethyl quinacridone (TM−DBQA), and *N*,*N*′-di(*n*-butyl)-2,9-di(*tert*-butyl) quinacridone (D^{t}Bu−DBQA) were synthesized according to the procedures reported previously.[26] The samples for NMR were prepared by dissolving the *N*,*N*′-di(*n*-butyl) quinacridone derivatives in $CDCl_3$ to obtain the concentrations of 60 mM for DBQA and 30 mM for both TM−DBQA and D^{t}Bu−DBQA. The stock solutions were diluted with $CDCl_3$ to obtain the samples with concentrations in the ranges of 0.05−60 mM for DBQA and 0.25−30 mM for both TM−DBQA and D^{t}Bu−DBQA. The samples with different volume percentages of polar solvents DMSO-d_6, CD_3OD, and CD_3CN in $CDCl_3$ were prepared by adding an aliquot of the stock to each tube and adding various volumes of polar solvents and $CDCl_3$ to give a sample concentration of 7.3 mM (total sample volume of 0.6 mL) and appropriate volume percentages of polar solvents.

The 1D and 2D NMR spectra were recorded on a Bruker Avance 500 spectrometer with TMS as the internal standard. The ROESY spectra were acquired with mixing times of 500 ms to 1 s.

Results and Discussion

The three *N*,*N*′-di(*n*-butyl) quinacridone derivatives used in this study are shown in Scheme 1. Considering the molecular symmetry which gives rise to the same chemical shifts for H1 and H8, H2 and H9, H3 and H10, H4 and H11, and H6 and H13, we relabeled the molecules according to their symmetries (Scheme 1). The original labels[27] of the atoms 1−6 remain unchanged, but the original atoms 8−13 (the numbers in parentheses in Scheme 1) are relabeled 1−6, respectively, in this study.

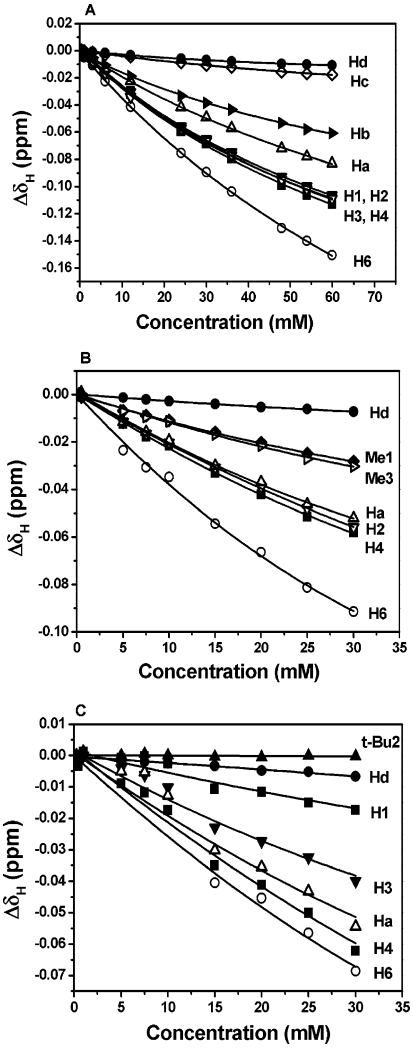

Figure 1. Concentration dependences of $\Delta\delta_H$ for DBQA (A), TM−DBQA (B), and D^{t}Bu−DBQA (C) at 298 K.

Aggregation with $\pi-\pi$ Stacked Interaction. It was observed during examination of the ^{1}H NMR spectra of the three quinacridone derivatives at various temperatures that the signals of all protons except for the *tert*-butyl groups of D^{t}Bu−DBQA shifted upfield with increasing concentrations of samples. Figure 1 demonstrates the concentration dependences of the ^{1}H peak shifts, $\Delta\delta_H$, relative to the corresponding resonances at the concentration of 0.25 mM for the three quinacridone derivatives in $CDCl_3$ at 298 K. When the temperature was decreased, all of the ^{1}H signals broadened gradually and split to two groups with different intensities at the temperatures of 228 and 213 K except for Hb, Hc, and Hd (Figure 2). The weight-averaged $\Delta\delta_H$ of the two groups of split signals for the three quinacridone derivatives as a function of concentration at 213 K are shown in Figure 3. The upfield shift of the ^{1}H signals with increasing concentration of sample indicates that the quinacridone derivatives aggregate with $\pi-\pi$ stacked interaction in solution.[8,9] The aggregation number *N*, i.e., the monomeric number included in an aggregate, was estimated by eq 1, assuming that the quinacridone derivatives are in equilibrium between the mono-

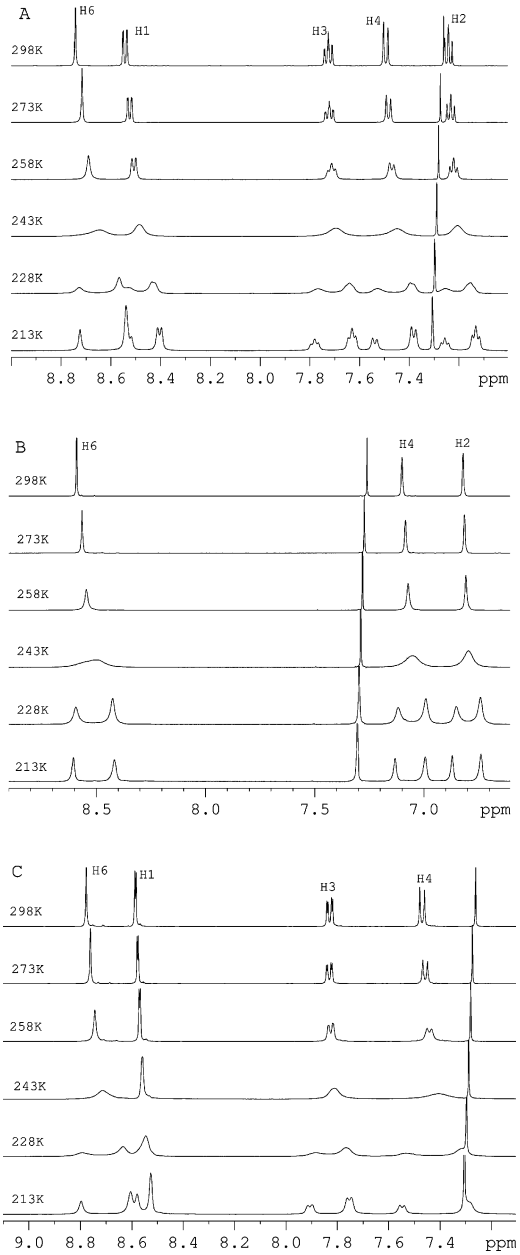

Figure 2. Aromatic regions of the ^{1}H spectra for DBQA (A), TM−DBQA (B), and D^{t}Bu−DBQA (C) at a concentration of 30.0 mM in $CDCl_3$ at various temperatures.

mer and the aggregate:[28]

$$\ln[C(\delta_m - \delta_{obs})] = N \ln[C(\delta_{obs} - \delta_{agg})] + \ln K + \ln N - (N-1)\ln(\delta_m - \delta_{agg}) \quad (1)$$

where δ_{obs} is the observed proton chemical shift and δ_m and δ_{agg} are the chemical shifts of the monomeric and aggregated molecules, respectively. C represents the total concentration, and K is the association constant. The plots of $\ln[C(\delta_m - \delta_{obs})]$ versus $\ln[C(\delta_{obs} - \delta_{agg})]$ may in principle give the aggregation number from the slope of the straight line and association constant K from the intercept of the line if δ_m and δ_{agg} are known. In practice, δ_m can be estimated from the chemical shifts of the samples diluted to very low concentrations, at which the quinacridone derivatives are considered as monomers. In contrast, the δ_{agg} is difficult to obtain in such a monomer−aggregate equilibrium process. However, it is naturally inferred

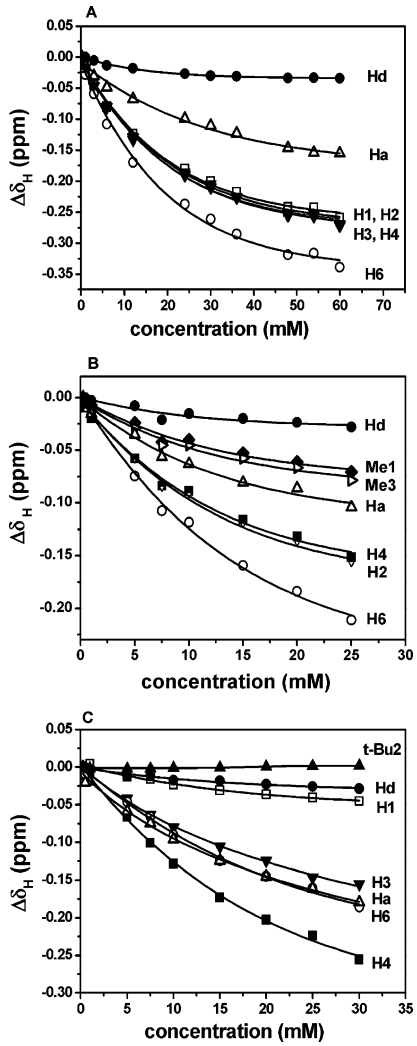

Figure 3. Concentration dependences of the weight-averaged $\Delta\delta_H$ for DBQA (A), TM−DBQA (B), and D^{t}Bu−DBQA (C) at 213 K.

that the candidate values of δ_{agg} must be those smaller than the chemical shifts of the samples at the highest concentrations. After testing a series of the values as δ_{agg} to plot $\ln[C(\delta_m - \delta_{obs})]$ versus $\ln[C(\delta_{obs} - \delta_{agg})]$, we found that there was a limit value. Any chemical shifts larger than the limit value as δ_{agg} lead to the dependence of $\ln[C(\delta_m - \delta_{obs})]$ versus $\ln[C(\delta_{obs} - \delta_{agg})]$ departing from straight lines, while using the chemical shifts smaller than the limit value as δ_{agg}, one can obtain straight lines with the slopes of ca. 2. This indicates that the values of δ_{agg} should not be larger than the limit and the values smaller than the limit have little effect on the dependence of $\ln[C(\delta_m - \delta_{obs})]$ versus $\ln[C(\delta_{obs} - \delta_{agg})]$ for the samples in the studied conditions. According to this method, we plotted the $\ln[C(\delta_m - \delta_{obs})]$ versus $\ln[C(\delta_{obs} - \delta_{agg})]$ for the samples of DBQA, TM−DBQA, and D^{t}Bu−DBQA at various temperatures using the chemical shifts of H4. For all the samples in the studied conditions (the concentrations and temperatures), the aggregation numbers of 2 were obtained. We also used the chemical shifts of H6 to plot the $\ln[C(\delta_m - \delta_{obs})]$ versus $\ln[C(\delta_{obs} - \delta_{agg})]$ for the three quinacridone derivatives at various temperatures and obtained similar results.

Association Thermodynamics. The concentration dependences of the ^{1}H chemical shifts at various temperatures for the three quinacridone derivatives in $CDCl_3$ were used to estimate the association constants (K) based on eq 2 if we assume that monomer−dimer equilibrium is the predominant process of the

TABLE 1: Association Constants for the Three Quinacridone Derivatives in $CDCl_3$ at Various Temperatures

	K (M^{-1})[a]		
T (K)	DBQA	TM−DBQA	D^{t}Bu−DBQA
298	3.2 ± 0.3	2.3 ± 1.2	1.9 ± 1.9
288	3.9 ± 0.4	3.1 ± 1.1	2.3 ± 1.5
273	6.5 ± 1.0	4.3 ± 1.4	6.4 ± 3.1
258	8.4 ± 0.7	5.3 ± 1.3	7.7 ± 4.9
243	10.0 ± 0.4	6.4 ± 0.3	3.8 ± 1.3
228	14.9 ± 0.7	12.6 ± 1.8	7.3 ± 1.9
213	20.6 ± 2.0	17.9 ± 2.9	11.4 ± 1.7

[a] The K values were obtained from δ_{H4}.

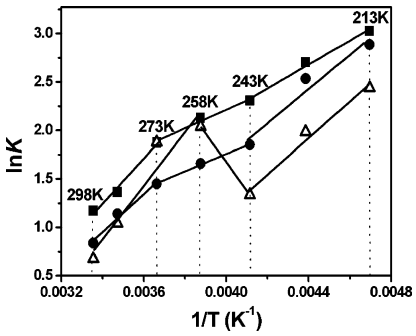

Figure 4. van't Hoff plots for DBQA (■), TM−DBQA (●), and D^{t}Bu−DBQA (△).

TABLE 2: Thermodynamic Parameters for the Self-Associations of the Three Quinacridone Derivatives in $CDCl_3$ at Various Temperatures

sample	T (K)	ΔH (kJ·mol^{-1})	ΔS (J·mol^{-1}·K^{-1})	ΔG (kJ·mol^{-1})
DBQA	213−243	−10.3 ± 1.0	−22.9 ± 4.4	−5.4 ± 0.1 (213 K)
	243−273	−7.9 ± 1.1	−13.2 ± 4.2	−4.5 ± 0.0 (258 K)
	273−298	−19.3 ± 2.2	−55.3 ± 7.8	−2.8 ± 0.1 (298 K)
TM−DBQA	213−243	−14.7 ± 3.3	−44.5 ± 14.5	−5.2 ± 0.2 (213 K)
	243−273	−7.4 ± 0.4	−15.1 ± 1.5	−3.5 ± 0.0 (258 K)
	273−298	−16.3 ± 2.2	−47.3 ± 7.7	−2.2 ± 0.1 (298 K)
D^{t}Bu−DBQA	213−243	−15.7 ± 2.2	−53.2 ± 9.8	−4.4 ± 0.1 (213 K)
	243−258	24.5 ± 0.0	111.7 ± 0.0	−4.4 ± 0.0 (258 K)
	258−298	−23.0 ± 4.9	−70.7 ± 17.5	−1.9 ± 0.4 (298 K)

self-association.[29]

$$\delta_{obs} = \delta_d + (\delta_d - \delta_m)\{[1 - (8KC + 1)^{1/2}]/(4KC)\} \quad (2)$$

where δ_{obs} is the observed chemical shift, δ_m and δ_d are the chemical shifts of monomer and dimer, respectively, and C is the total concentration. The association constants calculated by eq 2 are summarized in Table 1. The van't Hoff plots obtained from the data in Table 1 are displayed in Figure 4. Unexpectedly, the van't Hoff plots exhibit three different temperature dependences of ln(K) at the temperature ranges of 298−273, 273−243, and 243−213 K for DBQA and TM−DBQA, and 298−258, 258−243, and 243−213 K for D^{t}Bu−DBQA, respectively. The thermodynamic parameters for the dimerization of the three samples in the three temperature regions were calculated based on the van't Hoff plots (Table 2).

The temperature appears to have an evident effect on the association processes of these quinacridone derivatives. At the temperature regions studied, there are three different thermodynamic processes. In higher temperature regions (298−273 K for both DBQA and TM−DBQA, 298−258 K for D^{t}Bu−DBQA), the association processes are driven by enthalpy, so as in lower temperature regions (243−213 K for all the three samples). In the intermediate temperature region, the case is somewhat different. Although the association processes are also driven by the enthalpy for DBQA and TM−DBQA in this temperature region (273−243 K), the increases in ln(K) versus 1/T are slightly slower and the entropy values are less negative (Table 2). This indicates that the structures of the aggregates at this temperature region are less compact and thus more easily disassociated. This equilibrium transition is more obvious for D^{t}Bu−DBQA, in which the disassociation process occurs from 258 to 243 K, as indicated by both the positive entropy and enthalpy values (Table 2). This is attributed to the steric hindrance of the larger size of *tert*-butyl groups. As consequence, it is suggested that there exists a process of the conformational transition from higher temperature to lower temperature. Beyond the temperature region of the conformational transition, the self-associations are driven by enthalpy. However, within the transition region, the contribution of entropy to the self-association increases with increasing size of substituents on the aromatic rings. The transition processes are driven from by enthalpy for DBQA to by entropy for D^{t}Bu−DBQA, i.e., from unfavored entropy for DBQA to favored entropy for D^{t}Bu−DBQA. Therefore, we believe that the geometries of the $\pi-\pi$ stacking of the three quinacridone derivatives are modulated more or less from higher temperature to lower temperature; the larger the substituent, the larger the modulation of the geometries.

SCHEME 2: Monomer/Dimer Equilibria

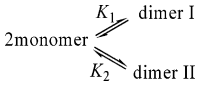

As mentioned above, with decreasing temperature, the ^{1}H signals broadened and split into two groups with different intensities at the temperatures lower than 243 K for the three quinacridone derivatives (Figure 2). Both the two groups of split signals at lower temperatures shifted upfield with increasing sample concentrations, in which the upfield parts of the doublets (assigned as group II) displayed a more rapid upfield shift with concentration than the downfield parts (assigned as group I). The intensities of the two groups of signals were also changed with sample concentration; the relative intensities of the group I decreased and those of the group II increased with increasing concentration. The ROESY spectra at 213 K displayed the cross-peaks between the two groups of signals, and they were in-phase with the diagonal peaks for all of the three quinacridone derivatives. This reveals the existence of two self-association processes for the three quinacridone derivatives in $CDCl_3$ solution; the one corresponding to the upfield parts of the split signals has a larger association constant, and the other corresponding to the downfield parts has a smaller association constant. The assignment of monomer and dimer for the two separated groups of signals can be excluded because either the decrease in the intensities of the downfield parts of the doublets or the increase in the intensities of the upfield parts of the doublets with concentration are much slower than they should be in the monomer−dimer equilibrium. Therefore, two types of the geometries of the $\pi-\pi$ stacking are suggested for the three quinacridone derivatives, and they are exchanged between each other (as supported by the ROESY spectra). The exchange rate between the two types of dimers is much slower than the association rates between their own monomer and dimer. Because of the coexistence of two association processes with different association constants, as shown in Scheme 2, the apparent association constant K obtained by eq 2 is the sum of the association constants of the two processes.

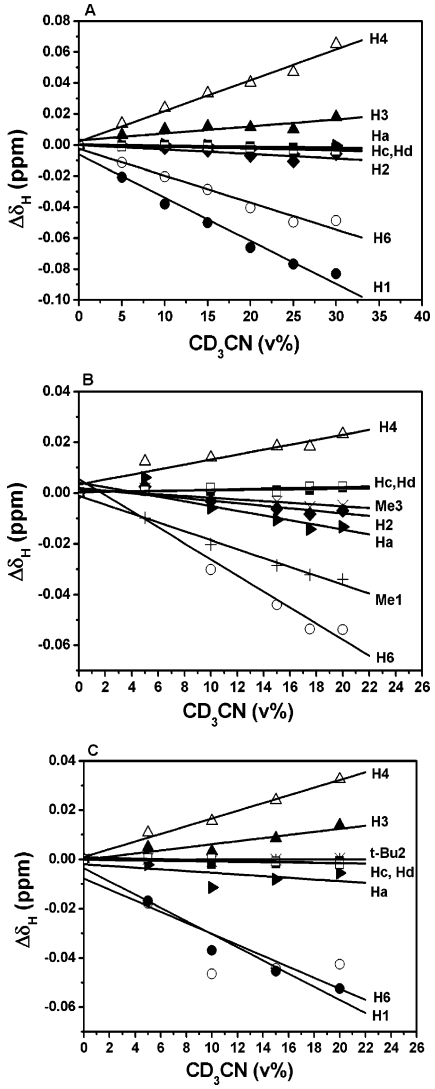

Figure 5. Peak shifts vs the volume percentage of CD_3CN in $CDCl_3$/CD_3CN mixture for DBQA (A), TM−DBQA (B), and D^{t}Bu−DBQA (C) at 298 K.

Effect of Solvent Polarity. When the polar solvents DMSO-d_6, CD_3CN, and CD_3OD, respectively, were added into $CDCl_3$ solutions of samples, the ^{1}H chemical shifts were changed. Depending on the positions of the protons in molecules, the chemical shifts were either increased or decreased or little changed with increasing fraction of the polar components. In general, the addition of the polar components in $CDCl_3$ resulted in evident upfield shifts of H1 and H6 and obvious downfield shifts of H4 for all the three samples. Moreover, the larger upfield shift of Me1 for TM−DBQA was also observed. The chemical shifts of the other protons were little affected by the polar solvents. Figure 5 illustrates the changes in the ^{1}H chemical shifts with the volume percentages of CD_3CN in the $CDCl_3$/CD_3CN mixtures for the three samples. The effect of the polar solvents on the chemical shifts is proportional to the dielectric constants of the polar solvents.

Geometries of $\pi-\pi$ Stacking. The patterns of the $\pi-\pi$ stacking for the three quinacridone derivatives in $CDCl_3$ can be estimated by the effects of polar solvents on the proton chemical shifts. With addition of DMSO-d_6, CD_3CN, and CD_3OD in $CDCl_3$, obvious upfield shifts of H6 and H1 resonances and downfield shifts of H4 resonances were observed for all the samples. This implies that the quinacridone derivatives may interact through the stacked fashions in which the carbonyl groups of one molecule are close to the nitrogen atoms of the partner molecules. The polar solvents induce the solvophobic interaction of the quinacridone derivatives and as a result increase the association constants and enhance the $\pi-\pi$ interaction, as indicated by previous investigations.[10,19,30] The enhancement of the $\pi-\pi$ interaction may make the π-electrons of the carbonyl groups and the lone-pair electrons of the nitrogen atoms of the partner molecules contact more closely. As a consequence, both the abilities of the electron-drawing of the carbonyl groups and the electron-giving of the nitrogen atoms may be decreased, which gives rise to the upfield shifts of H6 and H1 and the downfield shifts of H4 relative to the chemical shifts of the corresponding protons in pure chloroform.

TABLE 3: Peak Shifts of the Group I for the Three Quinacridone Derivatives from 0.25 to 25 mM at 213 K

	$\Delta\delta_{H-I}$ (ppm)					
sample	H1	H2	H3	H4	H6	Ha
DBQA	−0.11	−0.12	−0.09	−0.09	−0.12	−0.07
TM−DBQA		−0.08		−0.07	−0.10	−0.06
D^{t}Bu−DBQA	−0.01		−0.05	−0.07	−0.05	−0.06

TABLE 4: Peak Shifts of the Group II for the Three Quinacridone Derivatives from 0.25 to 25 mM at 213 K

	$\Delta\delta_{H-II}$ (ppm)					
sample	H1	H2	H3	H4	H6	Ha
DBQA	−0.22	−0.24	−0.24	−0.24	−0.30	−0.13
TM−DBQA		−0.21		−0.21	−0.29	−0.14
D^{t}Bu−DBQA	−0.06		−0.19	−0.31	−0.22	−0.29

The $\pi-\pi$ stacked geometries also can be estimated by the magnitudes of the peak shifts of protons, $|\Delta\delta_H|$. Because the observed chemical shifts are the weighted average of the proton resonances between the monomer and the dimer, as expressed in the eq 2, the $|\Delta\delta_H|$ is proportional to $|\delta_d - \delta_m|$. This means that the peak shift $\Delta\delta_H$ should reflect the locations of protons relative to the aromatic rings of the stacked partner if the ring current effect from the stacked partner is dominant for the peak shifts of all positions of protons. The peak shifts of aromatic protons and Ha arising from two different associations at 213 K are summarized in Tables 3 and 4. It is shown that the $|\Delta\delta_{H-I}|$ and $|\Delta\delta_{H-II}|$ possess similar order for different positions of protons in one molecule, i.e., the largest peak shift for H6, followed by the aromatic protons from the outer aromatic rings which are slightly different from each other, and finally Ha for both DBQA and TM−DBQA and the largest peak shift of H4, second-ranked Ha, followed by H6 and H3, and the smallest H1 for D^{t}Bu−DBQA. This means that the relative location of these protons in one association geometry is similar to that in the other association geometry. In addition, the stacked geometries of DBQA and TM−DBQA may be similar and somewhat different from those of D^{t}Bu−DBQA.

On the basis of the $\Delta\delta_H$ of two groups of split signals at 213 K as given in Tables 3 and 4, as well as the results of the polar solvents, we proposed a profile about the preferential geometries of the $\pi-\pi$ stacking for the three quinacridone derivatives in $CDCl_3$ at 213 K (Figure 6). In the profile, each of the three samples forms two preferential stacked patterns, I and II. In pattern I, the monomers are face-to-face stacked in a parallel fashion and alternately slipped two rings relative to one another along with the long axes of the conjugated ring systems. In pattern II, the monomers are also face-to-face stacked but in an antiparallel or a turning fashion with slight slipping between layers. The common characteristics of these stacked geometries is that the nitrogen atoms in one molecule as electron donors approach the carbonyl groups in the stacked partner as electron

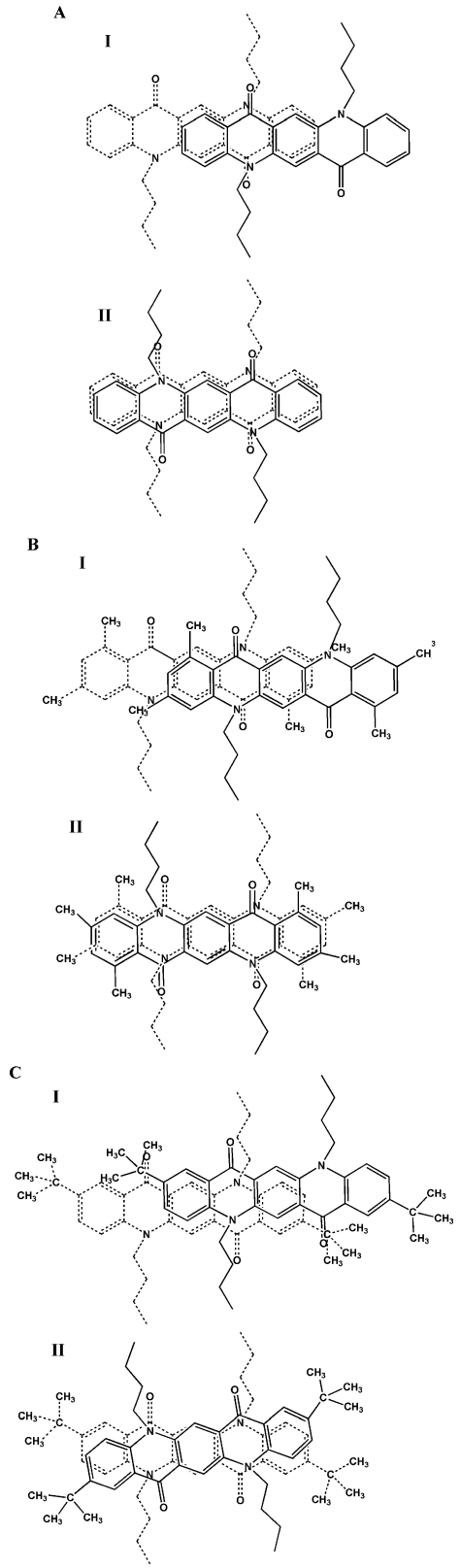

Figure 6. Proposed $\pi-\pi$ stacking models for DBQA (A), TM−DBQA (B), and D^{t}Bu−DBQA (C) in solution at 213 K.

acceptors and the electron-deficient atoms prefer to stack with both the electron-rich and electron-deficient atoms of the partner molecule, maximizing electrostatic complementary.[13] The *n*-butyl groups on the N atoms extend out of the stacked columns. The size of substitutes on the outer aromatic rings affects the geometry of the $\pi-\pi$ stacking significantly. The methyl groups of TM−DBQA make the interacted molecules more distant

TABLE 5: Peak Shifts for the Three Quinacridone Derivatives from 0.25 to 25 mM at 298 K

	$\Delta\delta_H$ (ppm)					
sample	H1	H2	H3	H4	H6	Ha
DBQA	−0.06	−0.06	−0.06	−0.06	−0.08	−0.04
TM−DBQA		−0.05		−0.05	−0.08	−0.04
D^{t}Bu−DBQA	−0.01		−0.03	−0.05	−0.06	−0.04

TABLE 6: Peak Shifts for the Three Quinacridone Derivatives from 0.25 to 25 mM at 213 K

	$\Delta\delta_H$ (ppm)					
sample	H1	H2	H3	H4	H6	Ha
DBQA	−0.18	−0.19	−0.19	−0.18	−0.24	−0.12
TM−DBQA		−0.15		−0.15	−0.21	−0.10
D^{t}Bu−DBQA	−0.04		−0.15	−0.22	−0.16	−0.17

compared with DBQA, but the stacked geometries maintain less changed. However, the *tert*-butyl groups of D^{t}Bu−DBQA not only result in further increase in the distance between stacked molecules but give rise to relatively larger slipping (pattern I) or turning (pattern II) of the stacked molecules relative to one another as well to avoid steric hindrance of the bulky groups. This regulation in aggregate conformation at 213 K puts H4 and Ha in more shielded positions of the stacked partner (i.e., H4 and Ha are more close to the upper position of the aromatic rings of the stacked partner) and thus lead to the unusually large peak shifts of H4 and Ha.

The solution structures of DBQA and TM−DBQA given above are different from their crystal structures except for the pattern I of DBQA that is consistent with its crystal structure.[26] As pattern I, DBQA in the crystal structure also adopts a stepped face-to-face stacking in a parallel fashion to form a column and the molecules in the column are alternately slipped two rings relative to one another along with the direction parallel to the long axis of the conjugated ring system. The molecular columns in the crystal are held together through weak intermolecular hydrogen bonding interactions between oxygen atoms on C═O groups and hydrogen atoms on outer phenyl rings. In the crystal structure of TM−DBQA, the molecules form a column by face-to-face stacking in a parallel fashion with little slipping between layers. The weak intermolecular hydrogen bonds between the oxygen atoms on C═O groups and the hydrogen atoms on CH_3 groups fix the column array. As we have known, the molecules in a crystal will attempt to achieve the arrangements which will result in the greatest intermolecular interactions and, consequently, the maximum lattice energy. Therefore, the specific arrangements or orientations adopted by a crystal structure depend on the summation of the lattice energies from various interactions. Although the molecular orientations in the stacked columns may be unfavorable to the electrostatic energy for the crystal structure of TM−DBQA, the disadvantage may be compensated by the favorable hydrogen-bonding interactions between the stacked columns. This means that an energy unfavorable stacking may be formed in the crystal structure if the arrangement of the stacked column can lead to more favorable intermolecular interactions between columns and finally maximize the total lattice energy. Different from the crystal structures, however, the interactions between the stacked columns have little contributions to the stacked geometries in solution. The $\pi-\pi$ stacked patterns of the aggregates for these samples in solution may be controlled mainly by the electrostatic complementarity of the packing partners.

Comparing the weight-averaged values of the ^{1}H chemical shifts at 298 K to those at 213 K, one can find that the order of $|\Delta\delta_H|$ for different positions of protons in each sample is slightly

changed from 298 to 213 K despite the decrease in the magnitudes of all peak shifts at 298 K (Tables 5 and 6), indicating no intrinsic difference in the $\pi-\pi$ stacked geometries between the two temperatures. Therefore, it is suggested that the quinacridone derivatives also aggregate at 298 K with two types of geometries similar to those at 213 K. However, it is worth noticing that, whereas the upfield shifts of H4 and Ha of D^{t}Bu−DBQA are smaller than or equal to those of DBQA at 298 K, the upfield shifts of H4 and Ha of D^{t}Bu−DBQA are larger than those of DBQA at 213 K, indicating that the slipping or turning between the stacked partners at 298 K may be smaller than that at 213 K for D^{t}Bu−DBQA.

Conclusions

The three quinacridone derivatives studied aggregate in chloroform to dimers through the $\pi-\pi$ stacked interaction. The association thermodynamics was unusually changed at different temperature regions possibly owing to the regulations of the stacked structures. Although the structural regulations are very small from higher temperature to lower temperature, they are not directly achieved by the mutual shift or turning without the variation in the contact distance. The intermediate conformations may be necessary for the structural regulation. In the intermediates, the $\pi-\pi$ interactions are weaker and the structures are less compact, which gives rise to even a partial disassociation of the aggregates. The geometries of the $\pi-\pi$ stacking in aggregates can be estimated by both the magnitudes of peak shifts with concentration and the directions of peak shifts induced by polar solvents. For the three quinacridone derivatives studied here, the solution structures of the $\pi-\pi$ stacking adopt face-to-face fashions in which the electrostatic complementarity is maximized. The substituent size has an evident effect on the stacked geometries and the association thermodynamics. The larger size of the substituents can reduce the strength of the $\pi-\pi$ stacked interaction and change the geometry of the stacking and meanwhile largely change the thermodynamics of the self-association processes.

Acknowledgment. This work was financially supported by the National Basic Research Program of China (2003CB615802, 2002CB613401), the National Natural Science Foundation of China (50225313), and the PCSIRT (IRT0422).

References and Notes

(1) Hunter, C. A.; Lawson, K. R.; Perkins, J.; Urch, C. J. *J. Chem. Soc., Perkin Trans. 2* **2001**, 651.

(2) Watson, J. D.; Crick, F. H. *Nature* **1953**, *171*, 737.

(3) Saenger, W. *Principles of Nucleic Acid Structure*; Spinger-Verlag: New York, 1984.

(4) Burley, S. K.; Petsko, G. A. *Science* **1985**, *299*, 23.

(5) Burley, S. K.; Petsko, G. A. *Adv. Protein Chem.* **1988**, *39*, 125.

(6) Hunter, C. A.; Singh, J.; Thornton, J. M. *J. Mol. Biol.* **1991**, *218*, 837.

(7) Claessens, C. G.; Stoddart, F. *J. Phys. Org. Chem.* **1997**, *10*, 254.

(8) Zhang, J.; Moore, J. S. *J. Am. Chem. Soc.* **1992**, *114*, 9701.

(9) Shetty, A. S.; Zhang, J.; Moore, J. S. *J. Am. Chem. Soc.* **1996**, *118*, 1019.

(10) Tobe, Y.; Utsumi, N.; Kawabata, K.; Nagano, A.; Adachi, K.; Araki, S.; Sonoda, M.; Hirose, K.; Naemura, K. *J. Am. Chem. Soc.* **2002**, *124*, 5350.

(11) Gabriel, G. J.; Sorey, S.; Iverson, B. L. *J. Am. Chem. Soc.* **2005**, *127*, 2637.

(12) Lee, J.; Guelev, V.; Sorey, S.; Hoffman, D. W.; Iverson, B. L. *J. Am. Chem. Soc.* **2004**, *126*, 14036.

(13) Hunter, C. A.; Sanders, J. K. M. *J. Am. Chem. Soc.* **1990**, *112*, 5525.

(14) Sinnokrot, M. O.; Valeev, E. F.; Sherrill, C. D. *J. Am. Chem. Soc.* **2002**, *124*, 10887.

(15) Sinnokrot, M. O.; Sherrill, C. D. *J. Phys. Chem. A* **2003**, *107*, 8377.

(16) Sinnokrot, M. O.; Sherrill, C. D. *J. Phys. Chem. A* **2004**, *108*, 10200.

(17) Thetforda, D.; Cherrymanb, J.; Chorltonc, A. P.; Docherty, R. *Dyes Pigm.* **2004**, *63*, 259.

(18) Mckay, S. L.; Haptonstall, B.; Gellman, S. H. *J. Am. Chem. Soc.* **2001**, *123*, 1244.

(19) Cubberley, M. S.; Iverson, B. L. *J. Am. Chem. Soc.* **2001**, *123*, 7560.

(20) Rashkin, M. J.; Waters, M. L. *J. Am. Chem. Soc.* **2002**, *124*, 1860.

(21) Gabriel, G. J.; Iverson, B. L. *J. Am. Chem. Soc.* **2002**, *124*, 15174.

(22) Chen, M. J.; Rathke, J. W. *J. Porphyrins Phthalocyanines* **2001**, *5*, 528.

(23) Veinot, J. G. C.; Yan, H.; Smith, S. M.; Cui, J.; Huang, Q.; Marks, T. J. *Nano Lett.* **2002**, *2*, 333.

(24) Gross, E. M.; Anderson, J. D.; Slaterbeck, A. F.; Thayumanavan, S.; Barlow, S.; Zhang, Y.; Marder, S. R.; Hall, H. K.; Nabor, M. F.; Wang, J.-F.; Mash, E. A.; Armstrong, N. R.; Wightman, R. M. *J. Am. Chem. Soc.* **2000**, *122*, 4972.

(25) Flora, W. H.; Hall, H. K.; Armstrong, N. R. *J. Phys. Chem. B* **2003**, *107*, 1142.

(26) Ye, K. Q.; Wang, J.; Sun, H.; Liu, Y.; Mu, Z. C.; Li, F.; Jiang, S. M.; Zhang, J. Y.; Zhang, H. X.; Wang, Y.; Che, C. M. *J. Phys. Chem. B* **2005**, *109*, 8008.

(27) Lincke, G. *Dyes Pigm.* **2000**, *44*, 101.

(28) Taboada, P.; Attwood, D.; Ruso, J. M.; Garcia, M.; Sarmiento, F.; Mosquera, V. *Langmuir* **2000**, *16*, 3175.

(29) Martin, R. B. *Chem. Rev.* **1996**, *96*, 3043.

(30) Lahiri, S.; Thompson, J. L.; Moore, J. S. *J. Am. Chem. Soc.* **2000**, *122*, 11315.